

DISTRIBUTION OF FLUORESCENTLY LABELED ACTIN IN LIVING SEA URCHIN EGGS DURING EARLY DEVELOPMENT

YU-LI WANG and D. LANSING TAYLOR. From Cell and Developmental Biology, The Biological Laboratories, Harvard University, Cambridge, Massachusetts 02138

ABSTRACT

Rabbit skeletal muscle actin was labeled with 5-iodoacetamidofluorescein (5-IAF) and purified by gel filtration, ion-exchange chromatography, and polymerization-depolymerization. The resultant fluorescent conjugates retained full biochemical activities. The labeled actin was incorporated into unfertilized eggs of *Lytechinus pictus* by direct microinjection and the distribution of fluorescence was investigated after fertilization through the first division cycle. The results were interpreted by comparing the images with those of control eggs injected with fluorescein isothiocyanate (FITC)-labeled ovalbumin. After fertilization of eggs containing IAF actin, the membrane-cortical regions showed dramatic increases in fluorescence intensity which were not observed in FITC ovalbumin controls. During the first division, spindle regions of both IAF-actin-injected eggs and control eggs became distinctly fluorescent. However, no distinctly fluorescent contractile ring was detected in the cleavage furrow. After cytokinesis, the surface between blastomeres containing IAF actin exhibited an increase in fluorescence intensity. These observations have been compared with those of previous studies using different methods, and the possible implications have been discussed in relation to cellular functions.

KEY WORDS actin · early development · fertilization · fluorescence microscopy · sea urchin eggs · cytokinesis

Actin plays a fundamental role in several cellular processes during early development. After fertilization of sea urchin eggs, the cell cortex exhibits a dramatic structural transformation involving the assembly and reorganization of actin filaments (1, 3). During cell division, actin is involved in the formation and contraction of the contractile ring (18, 26), and a possible role of actin in chromosomal movements has also been suggested based on the identification of actin in the mitotic apparatus (4, 10, 25). Recent studies on sea urchin egg actin indicated that these possible functions are accomplished by a single species of actin (33, 34).

Unfortunately, further understanding of the functional activities of actin has been hampered by technical limitations. In contrast to that in

striated muscle, the microfilament systems in non-muscle cells are generally not well-organized, and the structures are usually transient in nature and sensitive to external manipulations. The static images obtained by most existing techniques such as immunofluorescence, fluorescent heavy meromyosin (HMM) labeling, or electron microscopy yield only limited information about the dynamic nature of actin in living cells. Moreover, the interpretation of the images has been complicated by several possible types of artifacts. It has been demonstrated that actin filaments are susceptible to improper fixation (20), while the images can be further distorted by detergent or glycerol extractions which remove soluble actin molecules. Labeling with fluorescent HMM or antibodies might impose another level of selectivity, depending on their interactions with different states and organizations of actin. Furthermore, the fluorescence intensity is affected by factors such as the total

path length and the distribution of membrane-bound organelles which limit the accessible volume for cytoplasmic actin. As a result, confusing results have been obtained, and it has been difficult to judge which image could best represent the overall distribution of actin in living nonmuscle cells (12).

The introduction of *in vivo* molecular cytochemistry suggested a possible new approach for studying the distribution and functions of specific proteins inside living cells (38). The procedure involves purifying the protein under study, labeling covalently with appropriate fluorophores, testing the conjugates for biochemical activities *in vitro*, and incorporating the fluorescent conjugates into living cells using microinjection techniques. Thus, the artifacts of fixation, selective extraction, and selective labeling are totally avoided. In the present investigation, this method has been used to study the dynamic distribution of fluorescently labeled actin inside living eggs of the sea urchin *Lytechinus pictus* from fertilization until completion of the first cleavage cycle. Possible artifacts caused by path length, distribution of organelles, and local ionic conditions have been identified by carrying out control experiments using fluorescein isothiocyanate (FITC)-labeled ovalbumin which was assumed to distribute uniformly in the accessible cytoplasm.

MATERIALS AND METHODS

Protein Labeling

Actin was purified from rabbit skeletal muscle by the method of Spudich and Watt (35). Fluorescent labeling using a sulfhydryl specific dye, 5-iodoacetamidofluorescein (5-IAF; Molecular Probes, Plano, Texas), was carried out essentially as described previously (38); however, 50 mM borate buffer (pH 8.5) was used instead of Tris-HCl buffer. The labeled F-actin was subsequently depolymerized and passed through a G-25 gel filtration column. Further purification was carried out by DEAE-cellulose ion-exchange chromatography (13) and one cycle of polymerization-depolymerization. The purified conjugate had a dye-to-protein molar ratio of 0.7–0.9 (using a molar extinction coefficient of 60,000 at 495 nm, pH 8.0 for bound fluorescein). Microinjections were carried out within 3 d of preparation. Ovalbumin was labeled using FITC (Sigma Chemical Co., St. Louis, Mo.) in carbonate-bicarbonate buffer at pH 9.5, and purified from unreacted FITC by G-25 gel filtration chromatography and repeated dialysis. The dye-to-protein molar ratio was estimated to be 1.6 (using a molar extinction coefficient of 68,000 at 495 nm, pH 8.0 for bound fluorescein). The stability of bound fluorophores

was tested by boiling the conjugates in 2% SDS, followed by gel filtration through a G-25 column which had been equilibrated with 2% SDS. A single fluorescent peak in the void volume was obtained for both labeled actin and ovalbumin, indicating that the fluorophores were covalently bound.

Microinjection

Eggs and sperm of the sea urchin *L. pictus* were obtained by intracoelomic injection of 0.55 M KCl. Eggs were treated with acidified seawater (pH 4.5) for 2 min to remove jelly coats, followed by repeated washes with normal sea water. The washed eggs were loaded into wedge-shaped microchambers and sealed with mineral oil (Fisher Scientific Co., Pittsburgh, Pa.). Microinjections were carried out essentially as described by Hiramoto (16). A buffer containing 2 mM piperazine-*N,N'*-bis(2-ethane sulfonic acid) (PIPES) pH 6.9–7.0, 0.2 mM ATP, 0.1 mM MgCl₂, and 0.1 mM dithiothreitol was used as the carrier solution, and up to ~5% egg volume was injected. The results were not affected by the amount of IAF actin incorporated. 5-IAF actin was injected in monomeric form at a concentration of 3–5 mg/ml; FITC ovalbumin was injected at a concentration of 3 mg/ml. The final average concentration of IAF actin in the cytoplasm was estimated to be <0.3 mg/ml, which represented ~10–15% of the average endogenous actin concentration (33, 34). The microinjection sometimes caused the formation of a nonfluorescent vesicle in the cytoplasm. However, if the size of the vesicle did not exceed ~1% egg volume, neither fertilization nor the first cell division was affected and the egg developed synchronously with uninjected eggs. After the injected protein had dispersed through the cytoplasm, the eggs were fertilized by releasing a suspension of sperm in the vicinity of the eggs with a microneedle. Microchambers were maintained at 20°C throughout the period of observation.

Image Observation and Recording

Injected eggs were observed with a Zeiss photomicroscope III (Carl Zeiss, Inc., New York) using both epifluorescence optics with 25× Neofluar objectives (NA 0.60) and Nomarski optics with 16× Planachromat objectives (NA 0.35). A 60-W quartz-halogen lamp was used as the light source. Injected eggs were maintained with minimum exposure to the excitation light (490 nm) until they reached the stages under investigation. This procedure minimized bleaching artifacts. Fluorescent images were recorded on Kodak Tri-X pan film with the automatic camera of the photomicroscope at ASA 3,200 or 1- to 1.5-min timed exposures.

RESULTS

IAF actin purified by DEAE ion-exchange chromatography maintained similar polymerizability and activated HMM Mg-ATPase to the same

extent as unlabeled actin. The fluorescence properties of bound fluorescein moieties have been studied by spectrofluorimetry. No significant change in fluorescence intensity was observed upon polymerization of actin or after changing the ionic strength. However, the fluorescence intensity of both IAF actin and FITC ovalbumin increased to the same extent when the pH was increased from 6.6 to 7.4. A detailed description of the fluorescence and biochemical properties of the labeled proteins will be published elsewhere.

The egg cytoplasm exhibited negligible autofluorescence when illuminated by the excitation light at 490 nm. No fluorescence image could be recorded from uninjected eggs under the conditions used for photographing injected eggs. Images of injected eggs were recorded before fertilization, after fertilization, during mitosis, during cytokinesis, and after completion of the first cleavage (see Fig. 1 *a–f* for Nomarski photographs of these stages).

Unfertilized Eggs

In eggs containing IAF actin, distinctly fluorescent spots were observed at the sites of needle penetration for an extended period time (Fig. 2 *a*, arrow), suggesting the participation of actin in the wound healing process (17, 39). Otherwise, no distinctly fluorescent structure could be detected. The pronucleus remained about as fluorescent as the surrounding cytoplasm and could not be discerned in the fluorescent images (Fig. 2 *a*). In contrast, FITC ovalbumin readily entered the pronucleus so that distinctly fluorescent pronuclei were observed (Fig. 2 *b*, arrow). The wound heal-

ing site, on the other hand, could not be detected in FITC ovalbumin controls.

Fertilization

Upon fertilization of eggs preloaded with IAF actin, dramatic increases in fluorescence intensity were observed in cortical regions. Within 4 min of fertilization, these eggs became surrounded by brightly fluorescent rims (Fig. 3 *a*). At this stage, the surfaces appeared to be uniformly fluorescent except for the sites of needle insertion. The high intensity of fluorescence in membrane-control regions remained for ~10 min and then gradually decreased. In FITC ovalbumin controls, no redistribution of fluorescence was observed during fertilization (Fig. 3 *b*), indicating that the formation of fluorescent rims was not caused by direct effects of local ionic conditions (ie. local increase in pH) on the fluorophores.

Mitosis and Cytokinesis

The mitotic spindle could be detected by Nomarski optics as a region free of large yolk granules (Fig. 1 *c*). Similar fluorescent images were obtained whether the eggs were preloaded with IAF actin or FITC ovalbumin (Fig. 4 *a* and *b*). In both cases, the mitotic spindle was clearly more fluorescent than the surrounding cytoplasm. During telophase, distinct fluorescence was also observed in interzonal regions (Fig. 5 *a* and *b*). In eggs containing IAF actin, the forming daughter nuclei appeared as two faintly fluorescent regions (Fig. 5 *a*, arrows); whereas no forming nuclei were seen in fluorescent images of FITC ovalbumin controls (Fig. 5 *b*).

The surfaces of eggs injected with IAF actin exhibited localized increases in fluorescence intensity before the first cleavage, to form many discrete fluorescent spots (Figs. 6 *a*, and 8 *a* and *b*). In FITC ovalbumin controls, no fluorescent surface structures were observed (Fig. 6 *b*).

The cleavage furrow appeared as a band of lower fluorescence intensity than the adjacent cytoplasm, probably because of the smaller path-length (Fig. 6 *a* and *b*). No distinctly fluorescent contractile ring was observed throughout cytokinesis in both IAF-actin-injected eggs and controls. However, some eggs containing IAF actin exhibited striking banding patterns perpendicular to the cleavage furrows (Fig. 8 *a* and *b*).

During cytokinesis, eggs injected with IAF actin became very sensitive to the excitation light. Prolonged illumination delayed the completion of

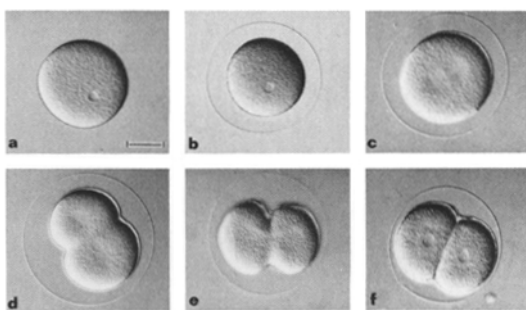


FIGURE 1 States of early development using Nomarski optics. (*a*) Unfertilized egg; (*b*) fertilized egg; (*c*) mitosis; (*d*) initiation of cytokinesis; (*e*) surface view of mid-cytokinesis; and (*f*) two-cell blastomeres. Corresponding fluorescent images are shown in Figs. 2–7. Bar, 50 μm . $\times 200$.

cytokinesis or even caused relaxation of the cleavage furrow, implicating the participation of IAF actin in the cleavage process. This effect was not observed in uninjected eggs or ovalbumin controls.

Daughter Nuclei and Cell-Cell Contact Region

In blastomeres containing IAF actin, the nuclei could be detected as two faintly fluorescent regions embedded in distinctly fluorescent perinuclear cytoplasm (Fig. 7a). On the other hand, the nuclei in ovalbumin controls were at least as fluorescent as the surrounding cytoplasm (Fig. 7b). Toward the end of cytokinesis, the two blastomeres flattened against each other and a close contact was established (Fig. 1f). In blastomeres containing IAF actin, the surface of contact exhibited a gradual increase in fluorescence intensity until it became intensely fluorescent (Fig. 7a). The high intensity persisted at least through the second division cycle. This phenomenon was never observed in ovalbumin controls (Fig. 7b).

DISCUSSION

Interpretation of Fluorescent Images

In interpreting the two-dimensional fluorescent image in terms of three-dimensional distribution of fluorophores, it is important to note that the fluorescent image represents a superposition of a focused image from a thin plane and defocused light emitted from other planes of the sample. Thus, the apparent distribution of fluorescence intensity is affected by both the plane of focus and the thickness (path length) of the sample. The light intensity is further affected by the distribution of those membrane-bound organelles which exclude the labeled protein. In regions of high organelle density, the fluorescence intensity would appear lower even though the concentration of the fluorophore is constant throughout the accessible cytoplasm. Local ionic conditions could also affect the intensity by altering the absorbance and/or quantum efficiency. Fluorescein, for example, is sensitive to pH.

In the present study, the problems of interpretation caused by the factors described above were solved by performing control experiments with FITC ovalbumin which was assumed to be distributed uniformly in the accessible cytoplasm. When recorded at the same plane of focus as that for eggs containing IAF actin, the images of FITC

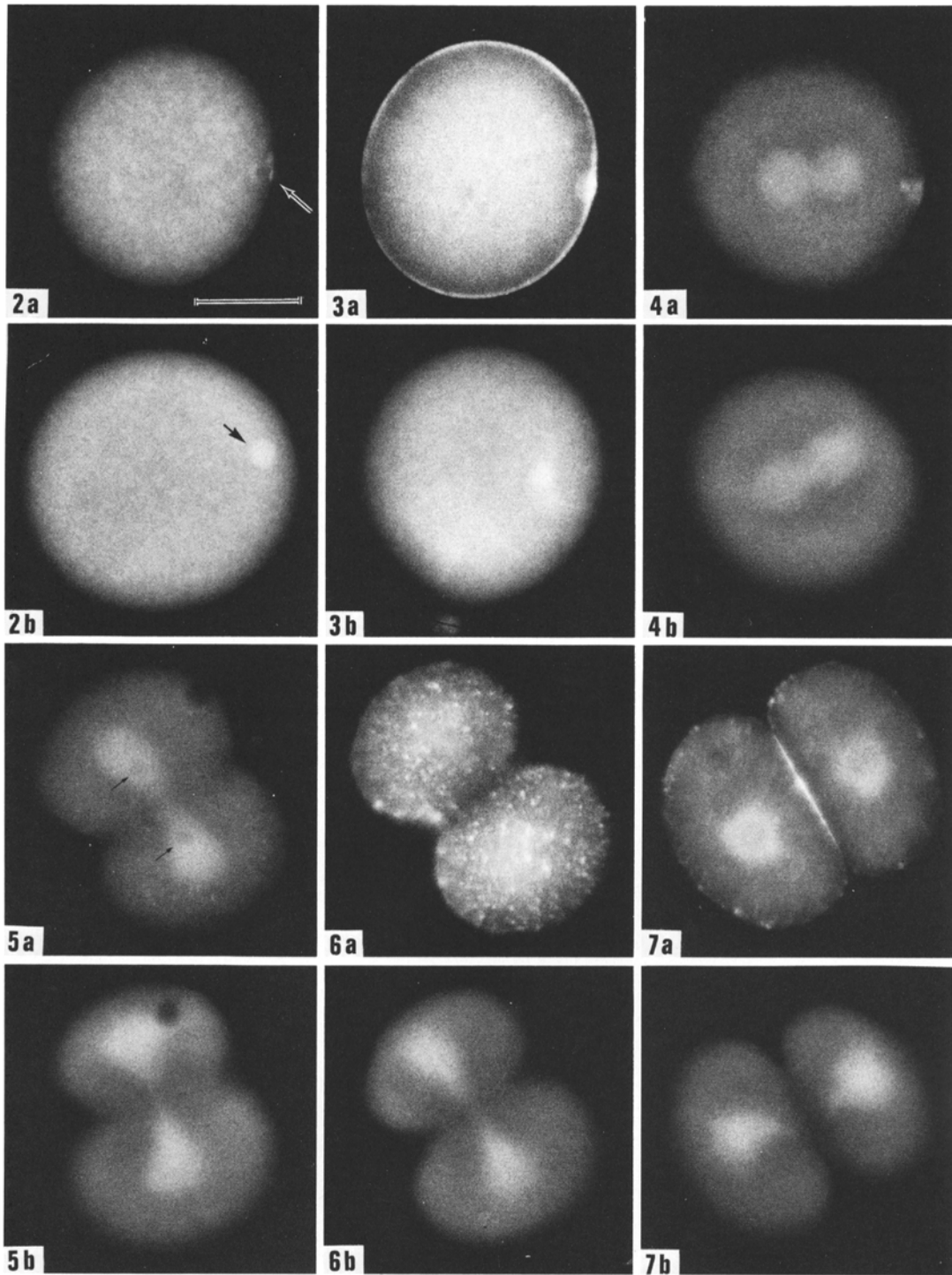
ovalbumin provided direct information on the effects of accessible cytoplasm, path length, and local ionic conditions on the distribution of fluorescence intensity in the eggs. Therefore, the differences in the distribution of fluorescence observed in eggs containing FITC ovalbumin and IAF actin reflected local variations in the actin concentration.

A parameter which can not be identified by the FITC ovalbumin control is the hydrophobicity of the microenvironment. Local conformational changes could be induced as a result of interactions between IAF actin and other proteins, resulting in different fluorescence intensities. However, this factor is not likely to alter our qualitative interpretation in view of the limited microenvironmental sensitivity of IAF observed on other proteins (14, 44), and the small microenvironmental change at sulfhydryl groups of actin reported previously (19, 30). While our preliminary data indicated no significant change in fluorescence intensity during polymerization, effects of interactions with myosin and actin-binding proteins are possible and these are now under investigation *in vitro*.

Cortical Actin

The transient increase in actin concentration in plasma membrane-cortical regions during fertilization is probably directly related to the structural transformation of the cell surface and cortex. Upon fertilization, there is a transient elongation of surface microvilli (3, 8, 28) along with a transient increase in the rigidity of the cortex (21). Our observations are consistent with previous ultrastructural studies which showed dramatic increases in the number of microfilaments both inside microvilli and in cortical regions (1, 3). Whether the number of cortical microfilaments decreases subsequently remains to be investigated. A transient increase in cytoplasmic free calcium concentration and pH has also been detected during fertilization (9, 11, 31, 36). In view of the possible role of calcium and pH in triggering actin polymerization (40) and cytoplasmic contractions (6, 23), similar processes might occur in the cortex to cause dramatic changes in actin concentration and the transformation of cortical properties.

The formation of membrane-associated fluorescent spots before cleavage could be related to the second burst of microvilli elongation which involves ~10–25% of the surface microvilli (27). In addition, an elongation of the "attachment fibers"



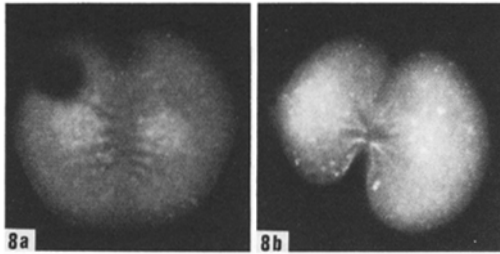


FIGURE 8 Fluorescent banding patterns on the surface of cleavage furrows are observed in some eggs containing IAF actin during early cytokinesis (a) and late cytokinesis (b). $\times 400$.

has also been reported in *Mespilia globulus* eggs "a few minutes before the onset of cleavage" (7). Future investigations using a combination of fluorescence techniques and electron microscopy on the same samples (22) should permit the absolute identification of these structures.

Although the role of actin during cytokinesis has been well demonstrated (see reference 26 for a review), it is still controversial whether the concentration of actin in the contractile ring is significantly higher than in other regions of the cell. While previous observations using fluorescent HMM labeling (25) and immunofluorescence (4) demonstrated an apparent concentration of actin in the cleavage furrow, a more recent report using fluorescent HMM indicated that the distribution of actin is more or less uniform in dividing cells (15).

The simplest interpretation of our results suggests that an extensive translocation of actin does not occur during the cleavage of sea urchin eggs. (However, a slight increase of actin concentration in the contractile ring might be difficult to detect because the path length of the cleavage furrow decreases during cytokinesis.) This interpretation is consistent with the results of Herman and Pollard (15), and would support a mechanism which involves a reorganization of actin filaments originally present in the equatorial cortex, probably including those located inside microvilli (37). Therefore, the local concentration of actin in the contractile ring obviously deserves further investigation. The effects of other contractile proteins on IAF actin fluorescence must be investigated before the fluorescence data can be interpreted unambiguously.

The cause of the banding patterns observed perpendicular to the cleavage furrows (Fig. 8) remains unknown. They might correspond to the membrane folds observed previously in *Aequorea* eggs (37), or could be formed by linear arrays of microvilli. Alternatively, it is also possible that microfilament bundles exist in the cortices perpendicular to the cleavage furrows. It will be interesting to find out whether the banding pattern is induced passively by the tension or plays some active role during cytokinesis.

The bright fluorescence on the proximal margins of daughter blastomeres indicated that a local

FIGURE 2 Fluorescent image of an unfertilized egg which has been microinjected with IAF actin (a), showing the wound healing response at the site of needle insertion (arrow). The pronucleus is invisible. FITC ovalbumin controls (b) do not show the wound healing site; however, the pronucleus is distinctly fluorescent (arrow). Bar, 50 μm . $\times 400$.

FIGURE 3 After fertilization, eggs preloaded with IAF actin (a) show a dramatic increase in fluorescence intensity near the plasma membrane; ~ 4 min after fertilization. FITC ovalbumin controls (b) do not show redistribution of fluorescence. $\times 400$.

FIGURE 4 In both eggs microinjected with IAF actin (a) with FITC ovalbumin (b), the mitotic apparatus is more fluorescent than the surrounding cytoplasm. $\times 400$.

FIGURE 5 During telophase, forming daughter nuclei are visible in eggs containing IAF actin (a, arrows), but not in eggs containing FITC ovalbumin (b). The interzonal regions are fluorescent in both images. $\times 400$.

FIGURE 6 During mid-cytokinesis, numerous fluorescent spots are visible on the the surfaces of eggs microinjected with IAF actin (a), but the furrow regions are not distinctly fluorescent. No distinct surface structure is visible in FITC ovalbumin controls (b). $\times 400$.

FIGURE 7 In blastomeres containing IAF actin (a), the nuclei are less fluorescent than the surrounding cytoplasm. However, the proximal margins of daughter blastomeres become brightly fluorescent. In FITC ovalbumin controls (b), both nuclei and cell-cell junctions are not discernable. $\times 400$.

concentration of actin is involved in the establishment and maintenance of cell-cell junctions. Previous observations have shown large numbers of interdigitating microvilli or filopodia between flattening blastomeres of sea urchin embryos (41). Scanning electron microscopy has also demonstrated numerous long microvilli between reaggregating sea urchin blastomeres (32). It is possible that the proximity of blastomeres triggers the formation or elongation of actin-containing microvilli. Subsequent associations between the microvilli followed by contractions would not only establish a close apposition but also generate force to flatten the blastomeres (42).

Mitotic Apparatus and Nuclear Actin

The fluorescent images of mitotic eggs indicated that actin is present in the mitotic apparatus. However, in view of the similar results with FITC ovalbumin, this observation must be interpreted with great caution. The apparent high intensity of FITC ovalbumin fluorescence is probably caused by the exclusion of large membrane-bound organelles from the mitotic apparatus, resulting in a large "accessible volume" for FITC ovalbumin. The pattern of distribution during telophase and in blastomeres is also consistent with this interpretation. Without further information, it is impossible to decide whether actin is playing an active role in the chromosomal movements, or is just passively present in the mitotic apparatus like ovalbumin. Because most soluble proteins, including myosin, could be present in the mitotic apparatus, the actual role of actin-myosin interactions during mitosis would depend on the organization and the ionic environment of the spindle. These results emphasize that the mere presence of a component does not necessarily imply function.

It has been previously demonstrated that microinjected ovalbumin enters the nucleus of frog oocytes and reaches a relatively uniform distribution between the nucleus and the accessible cytoplasm (2). The high fluorescence intensity observed in our experiment could be caused by either high pH of the nucleoplasm (5) or large accessible space inside the nucleus (2). If the images of FITC ovalbumin represent a relatively uniform distribution, the images of IAF actin would suggest a lower intranuclear actin concentration than the actin concentration in the accessible cytoplasm. The results could be explained if part of the injected actin was not in a freely diffusible form (ie. gel or F-actin) while the re-

maining actin would be unbound and capable of diffusing into nuclei.

Our results indicate that, using the technique of *in vivo* molecular cytochemistry, it is possible to study the dynamic distribution of specific biological molecules inside living cells. This technique not only allows direct verification of previous observations on fixed cells, but also yields important dynamic information otherwise difficult to obtain. The flexibility of the technique also points out new experimental approaches applicable to cell biological problems. For example, electron microscopy can be performed on microinjected cells to yield more detailed information about the fluorescent structures. The fluorescent images can be recorded using TV image intensification to minimize photobleaching (24, 29, 39, 43; Wang and Taylor, manuscript in preparation), and further coupled with time-lapse techniques and digital image analysis to quantitate changes in fluorescence distribution. Furthermore, using microspectrofluorimetry, it should be possible to study molecular interactions such as actin polymerization and actin-myosin interactions inside living cells. Therefore, a direct connection between *in vitro* biochemistry and *in vivo* cell biology could become a reality.

The authors would like to thank Dr. J. Ruderman and Dr. R. Linck for many helpful suggestions and practical assistance, and Mr. J. Lupo for technical assistance. Dr. J. Dowling has generously provided us with a seawater tank. We also acknowledge V. Fowler, J. Heiple, H. Virgin, and Dr. J. LaFountain for critically reading the manuscript.

The research was supported by the Institute of Arthritis, Metabolism, and Digestive Diseases Research grant AM 18111, and a Research Career Development Award to Dr. Taylor. Y.-L. Wang is a predoctoral student in the program of Biophysics at Harvard University.

Received for publication 7 December 1978, and in revised form 1 March 1979.

REFERENCES

1. BEGG, D. A., and L. I. REBHUN. 1978. pH induced changes in actin associated with the sea urchin egg cortex. *J. Cell Biol.* **79**(2, Pt. 2): 274a. (Abstr.)
2. BONNER, W. M. 1975. Protein migration into nuclei I. Frog oocyte nuclei *in vivo* accumulate microinjected histones, allow entry to small proteins, and exclude large proteins. *J. Cell Biol.* **64**:421-430.
3. BURGESS, D. R., and T. E. SCHROEDER. 1977. Polarized bundles of actin filaments within microvilli of fertilized sea urchin eggs. *J. Cell Biol.* **74**:1032-1037.
4. CANDE, W. Z., E. LAZARIDES, and J. R. MCINTOSH. 1977. A comparison of the distribution of actin and tubulin in the mammalian mitotic spindle as seen by indirect immunofluorescence. *J. Cell Biol.* **72**:552-567.
5. CHAMBERS, R., and E. L. CHAMBERS. 1961. Explorations into the Nature of the Living Cell. Harvard University Press, Cambridge, Mass.

6. CONDEELIS, J. S., and D. L. TAYLOR. 1977. The contractile basis of amoeboid movement. V. The control of gelation, solation, and contraction in extracts from *Dictyostelium discoideum*. *J. Cell Biol.* **74**:901-927.
7. DAN, K., and T. ONO. 1952. Cyto-embryological studies of sea urchins. I. The means of fixation of the mutual positions among the blastomeres of sea urchin larvae. *Biol. Bull.* **102**:58-73.
8. EDDY, E. M., and B. M. SHAPIRO. 1976. Changes in the topography of the sea urchin egg after fertilization. *J. Cell Biol.* **71**:35-48.
9. EPEL, D. 1977. The program of fertilization. *Sci. Am.* **237**(5):128-138.
10. FORER, A. 1974. Possible roles of microtubules and actin-like filaments during cell division. In *Cell Cycle Controls*. G. M. Padilla, I. L. Cameron, and A. Zimmerman, editors. Academic Press, Inc., New York. 319-336.
11. GILKEY, J. C., L. F. JAFFE, E. B. RIDGWAY, and G. T. REYNOLDS. 1978. A free calcium wave traverses the activating egg of the medaka, *Oryzias latipes*. *J. Cell Biol.* **76**:448-446.
12. GOLDMAN, R. D., M. YERNA, and J. A. SCHLOSS. 1976. Localization and organization of microfilaments and related proteins in normal and virus-transformed cells. *J. Supramol. Struct.* **5**:155-183.
13. GORDON, D. J., E. EISENBERG, and E. D. KORN. 1976. Characterization of cytoplasmic actin isolated from *Acanthamoeba castellanii* by a new method. *J. Biol. Chem.* **251**:4778-4786.
14. HARTIG, P. R., N. J. BERTRAND, and K. SAUER. 1977. 5-Iodoacetamido fluorescein-labeled chloroplast coupling factor 1: Conformational dynamics and labeling-site characterization. *Biochemistry.* **16**:4275-4282.
15. HERMAN, I. M., and T. D. POLLARD. 1978. Actin localization in fixed dividing cells stained with fluorescent heavy meromyosin. *Exp. Cell Res.* **114**:15-25.
16. HIRAMOTO, Y. 1961. Microinjection of the live spermatozoa into sea urchin eggs. *Exp. Cell Res.* **27**:416-426.
17. JEON, K. W., and M. S. JEON. 1975. Cytoplasmic filaments and cellular wound healing in *Amoeba proteus*. *J. Cell Biol.* **67**:243-249.
18. KIEHART, D. P., S. INOUÉ, and I. MABUCHI. 1977. Evidence that force production in chromosome movement does not involve myosin. *J. Cell Biol.* **75**(2, Pt. 2):258a. (Abstr.)
19. LIN, T. I. 1978. Fluorimetric studies of actin labeled with dansyl aziridine. *Arch. Biochem. Biophys.* **185**:285-299.
20. MAUFIN-SZAMIER, P., and T. D. POLLARD. 1978. Actin filament destruction by osmium tetroxide. *J. Cell Biol.* **77**:837-852.
21. MITCHISON, J. M., and M. M. SWANN. 1955. The mechanical properties of the cell surface. III. The sea urchin egg from fertilization to cleavage. *J. Exp. Biol.* **32**:734-750.
22. OSBORN, M., R. E. WEBSTER, and K. WEBER. 1978. Individual microtubules viewed by immunofluorescence and electron microscopy in the same PtK2 cell. *J. Cell Biol.* **77**:R27-R34.
23. POLLARD, T. D. 1976. The role of actin in the temperature-dependent gelation and contraction of extracts of *Acanthamoeba*. *J. Cell Biol.* **68**:579-601.
24. REYNOLDS, G. T. 1972. Image intensification applied to biological problems. *Q. Rev. Biophys.* **5**:295-347.
25. SANGER, J. W., and J. M. SANGER. 1976. Actin localization during cell division. In *Cell Motility*. R. Goldman, T. Pollard, and J. Rosenbaum, editors. Cold Spring Harbor Laboratory, Cold Spring Harbor, N. Y. 1295-1316.
26. SCHROEDER, T. E. 1975. Dynamics of the contractile ring. In *Molecules and Cell Movement*. S. Inoué and R. E. Stephens, editors. Raven Press, Inc., New York. 334-352.
27. SCHROEDER, T. E. 1978. Microvilli on sea urchin eggs: a second burst of elongation. *Dev. Biol.* **64**:342-346.
28. SCHROEDER, T. E. 1978. The surface area of a fertilized urchin egg is much smaller than predicted. *J. Cell Biol.* **79**(2, Pt. 2):171a. (Abstr.)
29. SEDLACEK, H. H., H. GUNDLACH, and W. AX. 1976. The use of television cameras equipped with an image intensifier in immunofluorescence microscopy. *Behring Inst. Mitt.* **59**:64-70.
30. SEKINE, T., T. OHYASHIKI, M. MACHIDA, and Y. KANAOKA. 1974. Studies on calcium ion-induced conformation changes in the actin-tropomyosin-troponin system by fluorimetry. 4. Conformation changes around the fluorescence-labeled sulfhydryl group of actin. *Biochim. Biophys. Acta.* **351**:205-213.
31. SHEN, S. S., and R. A. STEINHARDT. 1978. Direct measurement of intracellular pH during metabolic derepression of the sea urchin egg. *Nature (Lond.)* **272**:253-254.
32. SPIEGEL, E., and M. SPIEGEL. 1977. A scanning electron microscopy study of early sea urchin reagggregation. *Exp. Cell Res.* **108**:413-420.
33. SPUDICH, A., and J. A. SPUDICH. 1979. Actin in the triton-treated cortical preparations of unfertilized and fertilized sea urchin eggs. *J. Cell Biol.* **82**. In press.
34. SPUDICH, J. A., and A. SPUDICH. 1979. In *Cell Motility: Molecules and Organization*. S. Hatano, H. Ishikawa, and H. Sato, editors. Univ. of Tokyo Press, Tokyo. In press.
35. SPUDICH, J. A., and S. WATT. 1971. The regulation of rabbit skeletal muscle contraction. I. Biochemical studies of the interaction of the tropomyosin-troponin complex with actin and the proteolytic fragments of myosin. *J. Biol. Chem.* **246**:4866-4871.
36. STEINHARDT, R., R. ZUCKER, and G. SCHATTAN. 1977. Intracellular calcium release at fertilization in the sea urchin egg. *Dev. Biol.* **58**:185-196.
37. SZOLLOSI, D. 1970. Cortical cytoplasmic filaments of cleaving eggs. A structural element corresponding to the contractile ring. *J. Cell Biol.* **44**:192-209.
38. TAYLOR, D. L., and Y. L. WANG. 1978. Molecular cytochemistry: Incorporation of fluorescently labeled actin into living cells. *Proc. Natl. Acad. Sci. U.S.A.* **75**:857-861.
39. TAYLOR, D. L., and Y. L. WANG. 1978. Functional distribution of actin in living amoebae. *J. Cell Biol.* **79**(2, Pt. 2):273a. (Abstr.)
40. TILNEY, L. G., D. P. KIEHART, C. SARDET, and M. TILNEY. 1978. Polymerization of actin. IV. Role of Ca⁺⁺ and H⁺ in the assembly of actin and in membrane fusion in the acrosomal reaction of echinoderm sperm. *J. Cell Biol.* **77**:536-550.
41. VACQUIER, V. D. 1968. The connection of blastomeres of sea urchin embryos by filopodia. *Exp. Cell Res.* **52**:571-581.
42. VACQUIER, V. D., and D. MAZIA. 1968. Twinning of sand dollar embryos by means of dithiothreitol. *Exp. Cell Res.* **52**:209-219.
43. WILLINGHAM, M. C., and I. PASTAN. 1978. The visualization of fluorescent proteins in living cells by video intensification microscopy (VIM). *Cell.* **13**:501-507.
44. ZUKIN, R. S., P. R. HARTIG, and D. E. KOSHLAND, JR. 1977. Use of distant reporter group as evidence for a conformational change in a sensory receptor. *Proc. Natl. Acad. Sci. U.S.A.* **74**:1932-1936.